Mechanics of Materials 14 (1993) 239–251
Elsevier

Asymptotic fields of mode I steady-state crack propagation in non-associative elastoplastic solids

Enrico Radi and Davide Bigoni

Istituto di Scienza delle Costruzioni, Facoltà di Ingegneria, University of Bologna, Bologna, Italy

Received 24 March 1992; revised version received 24 August 1992

The quasi-static, steady-state propagation of a crack running in an elastoplastic solid with volumetric-non-associative flow law is analyzed. The adopted constitutive model corresponds to the small strain version of that proposed by Rudnicki and Rice. The asymptotic crack-tip fields are numerically obtained for the case of the incremental theory with linear isotropic hardening, under mode I plane-stress conditions. A relevant conclusion of the study is that the singularity of the near-tip fields appears to be mainly governed by the flow-rule, rather than by the yield surface gradient.

1. Introduction

Non-associative flow-laws were introduced by Mróz (1963) and Mandel (1966) in order to describe the behavior of frictional materials. Since then, the non-associativity has been identified as a key feature in the modelling of the behavior of many materials of engineering importance. Here we may mention porous metals and metals showing the S–D effect (Drucker, 1973; Spitzig et al., 1976), plastics (Whitney and Andrews, 1967), concrete (Palaniswamy and Shah, 1974), ceramics (Chen and Reyes-Morel, 1986; Reyes-Morel and Chen, 1988), rocks and soils (see, e.g., Chen, 1980). Moreover, a remarkable sensitivity of predictions to non-associativity has been shown for many elastoplastic constitutive models. In particular, certain instability phenomena would be predicted at unrealistic stress levels if the associative flow-rule were adopted (Rice, 1980). These instability phenomena, e.g., surface instability (Hutchinson and Tvergaard, 1980; Horii and Nemat-Nasser, 1982), orange-peel (Rittel, 1990), localized deformations (Rice, 1976) and elastoplastic cavitation (Huang et al., 1991), develop just before failure. For instance, Torrenti and Benaija (1990) have experimentally observed that, for concrete and fiber-reinforced concrete, localization of deformation occurs immediately before the peak of the stress–strain curve in simple compression. In order to model this experimental evidence in terms of an elastoplastic continuum, a strong degree of non-associativity is to be introduced (Bigoni, 1992).

From the above discussion, it can be concluded that, for a better understanding of fracture mechanisms in elastoplastic solids, the effect of non-associativity should be investigated. In this sense, FE simulations of crack growth in ductile pressure-sensitive materials have been performed (see, e.g., Aoki et al., 1984; 1987; Needleman and Tvergaard, 1987; 1992), in which a formulation of non-associative elastoplasticity is adopted, based on the Gurson (1977) model. However, the only contribution regarding asymptotic analysis near the crack tip seems to be that of Nemat-Nasser and Obata (1990). The type of non-associativity introduced by these authors comes from a particular type of non-coaxiality of the plastic flow-mode tensor and the stress tensor. This assumption, together with the incompressibility condition, yields to equations with the same structure

Correspondence to: Dr. D. Bigoni, Istituto di Scienza delle Costruzioni, Facultà di Ingegneria, Università di Bologna, Viale Risorgimento 2, 40136 Bologna, Italy.

of those of the associative case. In that paper, it is interesting to note that the perfect plasticity assumption, together with the non-associativity, yields the appearance of stress discontinuities in the solution.

The analysis of mode I steady-state quasi-static and dynamic crack propagation has been deeply investigated in the case of the J_2-flow theory with linear hardening (Amazigo and Hutchinson, 1977; Ponte-Castañeda, 1987a,b; Achenbach et al., 1981; Östlund and Gudmundson, 1988; Ponte-Castañeda and Mataga, 1991), as well as in the perfect plastic case (Slepyan, 1974; Gao, 1987; Rice et al., 1980; Drugan et al., 1982; Rice, 1982; Gao and Nemat-Nasser, 1983). With the exception of the papers of Li and Pan (1990a,b) and Li (1992), where the static of a crack in a Drucker–Prager deformation theory has been analyzed, no asymptotic analyses are available on crack propagation in pressure-sensitive materials. In a previous paper (Bigoni and Radi, 1992), the mode I steady-state, quasi-static propagation has been studied for an elastoplastic material obeying the Drucker–Prager yield criterion with associative flow-rule under plane stress and plane strain conditions. In that paper, it was shown that the pressure-sensitivity turns out to have a strong influence on the traction and the octahedral stresses ahead the crack tip.

In the present paper, the effect of the non-associativity is analyzed in mode I propagation, adopting the small strain formulation of the constitutive model of Rudnicki and Rice (1975) and Nemat-Nasser and Shokooh (1980). The model is based on the Drucker–Prager (1952) yield surface with a volumetric non-associative flow rule. When the plastic potential corresponds to the Huber–von Mises yield function, the model reduces to a Jenike–Shield (1959) type model and, consequently, plastic flow occurs without volumetric changes. A finite-strain version of this model was proposed by Needleman and Rice (1978) as a simplified model for capturing the S–D effect in metals and was later used by Needleman (1979) to investigate the effects of non-associativity on bifurcations of a block in plane-strain compression. The model used in the present paper, has been thoroughly studied from the point of view of local stability criteria (Rudnicki and Rice, 1975; Needleman, 1979; Vardoulakis, 1981; Chau and Rudnicki, 1990; Bigoni and Hueckel, 1990; Bigoni and Zaccaria, 1992); nevertheless, it had never been used in the asymptotic analysis of crack propagation. The study has been restricted to the condition of plane-stress, steady-state, quasi-static crack propagation in linear isotropic hardening. Solutions are found that satisfy the full continuity of fields across the elastic–plastic boundaries. In the framework of the adopted constitutive model, the non-associativity is shown to reduce, at low hardening, the amplitude of the plastic sector ahead the crack tip. Moreover, the singularity of the stress and velocity fields near the crack tip is found to be strongly dependent on the flow-rule, and only weakly dependent on the yield surface gradient. Therefore, the non-associativity appears to be a dominant parameter in crack-propagation analyses.

2. Constitutive model

The small strain version is adopted of the isotropic elastoplastic model proposed by Rudnicki and Rice (1975) and Nemat-Nasser and Shokooh (1980). Isotropic linear hardening is assumed. The stress–strain relation writes:

$$\dot{\boldsymbol{\epsilon}} = \frac{1}{E}\left((1+\nu)\dot{\boldsymbol{\sigma}} - \nu(\operatorname{tr}\dot{\boldsymbol{\sigma}})\boldsymbol{I} + \frac{1}{h}\langle \boldsymbol{Q}\cdot\dot{\boldsymbol{\sigma}}\rangle \boldsymbol{P}\right), \tag{2.1}$$

in which ν is the Poisson ratio, E the elastic modulus, h the ratio between hardening modulus and E, the operator $\langle\ \rangle$ denotes the McAulay brackets, $\boldsymbol{Q}$ is the gradient of the yield function:

$$\boldsymbol{Q} = \frac{\mu}{3}\boldsymbol{I} + \frac{\boldsymbol{S}}{2\sqrt{J_2}}, \tag{2.2}$$

where $\boldsymbol{S}$ is the deviatoric stress and μ the parameter governing the pressure-sensitivity. Finally, $\boldsymbol{P}$ is the flow-mode tensor:

$$\boldsymbol{P} = \frac{\beta}{3}\boldsymbol{I} + \frac{\boldsymbol{S}}{2\sqrt{J_2}}, \tag{2.3}$$

where β is the parameter governing the non-associativity. Plastic flow can occur only when the stress point lies on the (Drucker–Prager) yield surface:

$$\sigma_e - \frac{3}{\mu + \sqrt{3}} k = 0, \tag{2.4}$$

where the hardening parameter k is $1/\sqrt{2}$ time the radius of the deviatoric section of the yield surface with the π-plane in the Haigh–Westergaard stress space and σ_e is the effective stress:

$$\sigma_e = \frac{3}{\mu + \sqrt{3}} \left(\frac{\mu}{3} \operatorname{tr} \boldsymbol{\sigma} + \sqrt{J_2} \right), \tag{2.5}$$

which reduces to the principal non-zero stress component in uniaxial traction. Note from (2.1) that *elastic unloading* occurs when $\boldsymbol{Q} \cdot \dot{\boldsymbol{\sigma}} < 0$. Moreover, in the case of mode III stress state, it can be noted that the constitutive equation (2.1) coincides with the J_2-flow theory. Deviatoric non-associativity would change the response (in respect to the J_2-flow theory) even for antiplane shearing conditions. The model reduces to that of Drucker–Prager when $\beta = \mu$, to a Jenike–Shield type model, when $\beta = 0$ and $\mu \neq 0$ and, finally, to the J_2-flow theory when $\beta = \mu = 0$.

In order to facilitate the comparisons with the results from the J_2-flow theory, it is important to remark that h is related to the ratio α between the tangent modulus G_t (of the shear stress–engineering strain curve) and the elastic shear modulus through the following equation:

$$\alpha = \frac{2(1+\nu)h}{1 + 2(1+\nu)h}. \tag{2.6}$$

Moreover, in the special case $\beta = \mu = 0$ and $\nu = 1/2$, α turns out to be equal to the ratio between the uniaxial tangent modulus and the elastic modulus E.

The model (2.1) has been widely adopted in the constitutive description of various brittle and ductile materials, such as high strength steels, porous metals, ceramics, plastics, concrete, rocks and soils. However, the crack-propagation analysis that will be developed in the present paper appears to be suitable for homogeneous materials. Therefore, the analysis may be considered a rough modelling of fracture in concrete, due to the size of the inhomogeneities which are not comparable with the representative scale length of a near-tip field. For metals showing the SD effect, parameter μ may range from 0 to 0.07 and β is approximately $1/15$ of μ (Spitzig et al., 1976). In plastics μ may arrive at the value 0.26 with $\beta \approx \mu/6$. Reyes-Morel and Chen (1986; 1988) reported $\mu = \beta = 0.69$ for zirconia-containing ceramics. Finally, μ may range between 0.4 and 1.0 and β between 0.2 and 0.5 for rocks (Rudnicki and Rice, 1975).

3. Governing equations

A Cartesian reference system is adopted, with the origin attached to the moving crack tip, the x_1-axis in the direction of crack propagation and the x_3-axis normal to the plane of non-zero stresses. The steady-state propagation condition implies:

$$\dot{(\ )} = -V(\ )_{,1}, \tag{3.1}$$

where V denotes the (constant) crack-tip speed and comma indicates differentiation. Moreover, for algebraic convenience, a cylindrical system (r, ϑ, x_3) is employed, having the origin located at the crack tip and the longitudinal axis coincident with x_3.

In cylindrical coordinates, the equilibrium equations become:

$$\begin{cases} (r\sigma_{rr})_{,r} + \sigma_{r\vartheta,\vartheta} - \sigma_{\vartheta\vartheta} = 0, \\ (r\sigma_{r\vartheta})_{,r} + \sigma_{\vartheta\vartheta,\vartheta} + \sigma_{r\vartheta} = 0. \end{cases} \tag{3.2}$$

The three non-zero stress components and the two in-plane velocities (v_r and v_ϑ) are assumed as unknown ($\dot{\epsilon}_{33}$ is determined from (2.1) as a function of the non-zero stresses). By substituting the strain compatibility relation $\dot{\boldsymbol{\epsilon}} = (\nabla \boldsymbol{v} + (\nabla \boldsymbol{v})^{\mathrm{T}})/2$ into (2.1) and using the steady-state

condition (3.1), three equations are obtained in the five unknowns σ_{rr}, $\sigma_{\vartheta\vartheta}$, $\sigma_{r\vartheta}$, v_r and v_ϑ:

$$\frac{E}{V}v_{r,r} = \left(1 + \frac{1}{h}Q_{rr}P_{rr}\right) \times \left(\frac{\sin\vartheta}{r}\sigma_{rr,\vartheta} - \cos\vartheta\,\sigma_{rr,r} - \frac{2}{r}\sin\vartheta\,\sigma_{r\vartheta}\right) - \left(\nu - \frac{1}{h}Q_{\vartheta\vartheta}P_{rr}\right) \times \left(\frac{\sin\vartheta}{r}\sigma_{\vartheta\vartheta,\vartheta} - \cos\vartheta\,\sigma_{\vartheta\vartheta,r} + \frac{2}{r}\sin\vartheta\,\sigma_{r\vartheta}\right) + \frac{2}{h}Q_{r\vartheta}P_{rr}\left(\frac{\sin\vartheta}{r}\sigma_{r\vartheta,\vartheta} - \cos\vartheta\,\sigma_{r\vartheta,r} + \frac{1}{r}\sin\vartheta(\sigma_{rr} - \sigma_{\vartheta\vartheta})\right), \quad (3.3a)$$

$$\frac{E}{Vr}(v_{\vartheta,\vartheta} + v_r) = \left(1 + \frac{1}{h}Q_{\vartheta\vartheta}P_{\vartheta\vartheta}\right) \times \left(\frac{\sin\vartheta}{r}\sigma_{\vartheta\vartheta,\vartheta} - \cos\vartheta\,\sigma_{\vartheta\vartheta,r} + \frac{2}{r}\sin\vartheta\,\sigma_{r\vartheta}\right) - \left(\nu - \frac{1}{h}Q_{rr}P_{\vartheta\vartheta}\right) \times \left(\frac{\sin\vartheta}{r}\sigma_{rr,\vartheta} - \cos\vartheta\,\sigma_{rr,r} - \frac{2}{r}\sin\vartheta\,\sigma_{r\vartheta}\right) + \frac{2}{h}Q_{r\vartheta}P_{rr} \times \left(\frac{\sin\vartheta}{r}\sigma_{r\vartheta,\vartheta} - \cos\vartheta\,\sigma_{r\vartheta,r} + \frac{1}{r}\sin\vartheta(\sigma_{rr} - \sigma_{\vartheta\vartheta})\right), \quad (3.3b)$$

$$\frac{E}{2V}\left(v_{\vartheta,r} + \frac{1}{r}(v_{r,\vartheta} - v_\vartheta)\right) = \left(1 + \upsilon + \frac{2}{h}Q_{r\vartheta}^2\right) \times \left(\frac{\sin\vartheta}{r}\sigma_{r\vartheta,\vartheta} - \cos\vartheta\,\sigma_{r\vartheta,r} + \frac{1}{r}\sin\vartheta(\sigma_{rr} - \sigma_{\vartheta\vartheta})\right) + \frac{1}{h}Q_{r\vartheta} \times \left[Q_{\vartheta\vartheta}\left(\frac{\sin\vartheta}{r}\sigma_{\vartheta\vartheta,\vartheta} - \cos\vartheta\,\sigma_{\vartheta\vartheta,r} + \frac{2}{r}\sin\vartheta\,\sigma_{r\vartheta}\right) + Q_{rr}\left(\frac{\sin\vartheta}{r}\sigma_{rr,\vartheta} - \cos\vartheta\,\sigma_{rr,r} - \frac{2}{r}\sin\vartheta\,\sigma_{r\vartheta}\right)\right]. \quad (3.3c)$$

Equations (3.2) and (3.3) form a system of five first order PDEs. Solutions are sought in the HRR form (Hutchinson, 1968a,b; Rice and Rosengren, 1968), i.e.,

$$\begin{aligned} v_r(r,\vartheta) &= V\underline{r}^s\frac{1}{s}y_1(\vartheta), \\ v_\vartheta(r,\vartheta) &= V\underline{r}^s\frac{1}{s}y_2(\vartheta), \\ \sigma_{r\vartheta}(r,\vartheta) &= E\underline{r}^s y_3(\vartheta), \\ \sigma_{rr}(r,\vartheta) &= E\underline{r}^s y_4(\vartheta), \\ \sigma_{\vartheta\vartheta}(r,\vartheta) &= E\underline{r}^s y_5(\vartheta), \end{aligned} \quad (3.4)$$

where s is the stress singularity coefficient and the bar under r denotes non-dimensionalization with respect to any length parameter. The form of solution (3.4) has been widely adopted in crack-propagation analyses (Achenbach et al., 1991; Östlund and Gudmundson, 1988; Ponte-Castañeda, 1987a; Ponte-Castañeda and Mataga, 1991). However, it is well-known (Ponte-Castañeda, 1987a) that the singularity s does not approach the limit corresponding to the perfect-

plasticity solution when the hardening modulus tends to zero. Unfortunately, perfect-plasticity solutions are not available for the problem of crack-propagation in the assumed elastoplastic solid and therefore conclusions are not drawn concerning values of hardening approaching zero.

Substitution of (3.4) into (3.2) and (3.3) yields a system of five first order ODEs in the form:

$$\boldsymbol{y}' = \boldsymbol{f}(\boldsymbol{y}, \vartheta, s, \sigma_e, \operatorname{sign}(\boldsymbol{Q}\cdot\dot{\boldsymbol{\sigma}})). \tag{3.5}$$

It should be noted that the form of the system depends on the sign of the plastic multiplier and on the value of the effective stress σ_e which indicate, respectively, elastic unloading and plastic reloading. System (3.5) writes:

$$y_3' = -(1+s)y_4 + y_5, \tag{3.6a}$$

$$y_5' = -(s+2)y_3, \tag{3.6b}$$

$$y_4' = \frac{1}{\Delta \sin\vartheta} \times \left[[y_1 + (2-\nu s)\sin\vartheta\, y_3 + s(y_4 - \nu y_5)\cos\vartheta] + \frac{\langle \underline{\Delta}\rangle}{\underline{\Delta}} \frac{1}{h}\left(\frac{\beta}{3} + \frac{2y_4 - y_5}{6\sqrt{\underline{J}_2}}\right) \times (\Theta_1 \sin\vartheta\, y_3 + s\Theta_2 \cos\vartheta)\right], \tag{3.6c}$$

$$y_1' = (1-s)y_2 - 2(1+\nu)s^2(\sin\vartheta\, y_4 + \cos\vartheta\, y_3) + \langle \underline{\Delta}\rangle \frac{s y_3}{h\sqrt{\underline{J}_2}}, \tag{3.6d}$$

$$y_2' = -y_1 - s\sin\vartheta[\nu y_4' + (s-2\nu)y_3] + s^2\cos\vartheta(\nu y_4 - y_5) + \langle \underline{\Delta}\rangle \frac{s}{h}\left(\frac{\beta}{3} + \frac{2y_5 - y_4}{6\sqrt{\underline{J}_2}}\right), \tag{3.6e}$$

where $1/h = 0$ if $\sigma_e < 3k/(\mu + \sqrt{3})$ and:

$$\Delta = 1 + \frac{1}{h}\left(\frac{\beta}{3} + \frac{2y_4 - y_5}{6\sqrt{\underline{J}_2}}\right) \times \left(\frac{\mu}{3} + \frac{2y_4 - y_5}{6\sqrt{\underline{J}_2}}\right), \tag{3.7}$$

$$\Theta_1 = (s+2)\frac{\mu}{3} + \frac{2(s-1)y_5 + (5s+4)y_4}{6\sqrt{\underline{J}_2}}, \tag{3.8}$$

$$\Theta_2 = \frac{\mu}{3}(y_4 + y_5) + \sqrt{\underline{J}_2}, \tag{3.9}$$

$$\underline{\Delta} = y_4' \sin\vartheta\left(\frac{\mu}{3} + \frac{2y_4 - y_5}{6\sqrt{\underline{J}_2}}\right) - y_3\Theta_1 \sin\vartheta - s\Theta_2\cos\vartheta, \tag{3.10}$$

$$\underline{J}_2 = \tfrac{1}{3}(y_4^2 + y_5^2 - y_4 y_5) + y_3^2. \tag{3.11}$$

Equations (3.6a) and (3.6b) have been derived from (3.2) and Eq. (3.6c) from (3.3a), by using (3.6a) and (3.6b). Equations (3.6) differ from the analogous equations of Bigoni and Radi (1992) because of the terms containing the plastic flow-mode parameter β. For high values of non-associativity, the parameter Δ defined by (3.7) might vanish at sufficiently small values of hardening. Therefore, the value of Δ has to be checked during the numerical integration of system (3.5). However, Δ was always found to be greater than zero in all performed numerical cases. The vanishing of Δ seems to be connected with the emergence of solutions presenting discontinuities in the field variables.

The boundary conditions are:

$$\begin{cases} y_2(0) = y_3(0) = y_4'(0) = 0, & (3.12a) \\ y_3(\pi) = y_5(\pi) = 0, & (3.12b) \end{cases}$$

where (3.12a) have been obtained from mode I symmetry and (3.12b) from the requirement of zero tractions on the crack surface. Moreover, by

using (3.12) into Eqs. (3.9), the following auxiliary conditions are obtained:

$$y_1(0) = -s\left[y_4(0) - \nu y_5(0) + \frac{1}{h} \times\left(\frac{\beta}{3} + \frac{2y_4(0) - y_5(0)}{2\sqrt{3[y_4^2(0) + y_5^2(0) - y_4(0)y_5(0)]}}\right) \times\left(\frac{\mu}{3}[y_4(0) + y_5(0)] + \sqrt{[y_4^2(0) + y_5^2(0) - y_4(0)y_5(0)]/3}\right)\right]. \tag{3.13}$$

$$y_1'(0) = y_5'(0) = 0, \tag{3.14}$$

$$y_3'(0) = -(1+s)y_4(0) + y_5(0). \tag{3.15}$$

From a comparison with the corresponding equations of Bigoni and Radi (1992), it may be noted that the non-associativity affects the form of the PDEs, as well as the boundary condition (3.13).

Possibility of plastic reloading on crack flanks has been taken into account by assuming that the path of the (moving) particles is rectilinear (Östlund and Gudmundson, 1988; Ponte-Castañeda, 1987a). Plastic reloading occurs when a particle reaches the same value of effective stress it had at elastic unloading. The angle corresponding to elastic unloading will be denoted by ϑ_1; hence, plastic reloading occurs at the angle ϑ_2 which satisfies the following equation:

$$\sigma_e(\vartheta_1)/(\sin\vartheta_1)^s = \sigma_e(\vartheta_2)/(\sin\vartheta_2)^s \quad \text{and} \quad \underline{\Lambda} > 0. \tag{3.16}$$

In the following, solutions are sought which satisfy the continuity of all fields. Thus, the following conditions are imposed across elastic–plastic boundaries:

$$[\![y_1]\!] = [\![y_2]\!] = \cdots = [\![y_5]\!] = 0, \tag{3.17}$$

where $[\![y_i]\!]$ denotes the jump of y_i. However, as was pointed out by Nemat-Nasser and Obata (1990), non-associativity opens the possibility to the appearance of jump discontinuities in the radial stress and in the strain components. In fact, the continuity of the stress and strain fields for steadily propagating surfaces has been proved under the hypotheses of associative flow and isotropic (positive) hardening only (Drugan and Rice, 1984; Drugan and Yinong, 1990; Narasimhan and Rosakis, 1987; Nemat-Nasser and Gao, 1988). Therefore, the solutions to the problem analyzed in this paper may not be unique. The possible discovery of discontinuous solutions at positive hardening could be interpreted as the key-tool to explain the appearance of highly localized near-tip deformation patterns like those studied by Vitek (1976), Riedel (1976) and Lo (1979).

4. Numerical results

In order to solve the system (3.6), subject to (3.12), the Runge–Kutta method is employed. The Runge–Kutta method requires the knowledge of all the values of functions y_i at $\vartheta = 0$. Therefore, the normalization $y_4(0) = 1$ is introduced and an initial estimate is given of the values of $y_5(0) = q$ and s. After the numerical integration is performed, a check is made to determine if conditions (3.12b) are satisfied. On the basis of the error made on (3.12b), new values of q and s are given; the integration is then re-started and the process is iterated until the solution is approached with the required accuracy. The scheme adopted for the iteration on q and s is the modified Powell hybrid method, used also by Östlund and Gudmundson (1988). Both the Runge–Kutta and Powell methods were available in the IMSL library (subroutines DIVPRK and DNEQNF). Finally, when q and s are determined, the solution is re-normalized by assuming $\sigma_e(\vartheta_1)/Er^s = 1$.

As in the case of the associative flow-rule, the influence of ν was found negligible and no reloading was observed. Therefore, all results are given for $\nu = 1/2$ and the angle ϑ_2 is never reported. In order to make comparisons easier, the plots of the angular distributions of the stress components for the J_2-flow theory are reported in Fig. 1, for $\alpha = 0.001$, and in Fig. 8, for $\alpha = 0.1$. It should be mentioned that the graphs reported

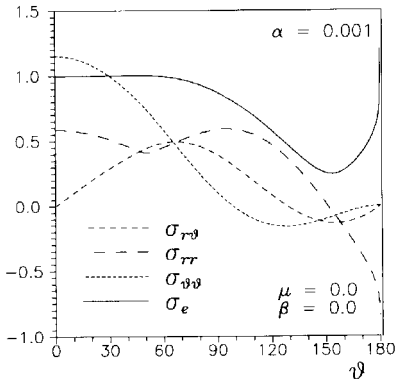

Fig. 1. Angular stress distribution for small strain hardening in the case of J_2-flow theory.

in Fig. 1 coincide with those of Fig. 16b in Ponte-Castañeda (1987). The values of the singularity s and of the unloading angle ϑ_1 are reported in Tables 1 and 2. The plots in all the figures represent the angular distributions of functions y_i ($-y_i$ for y_1 and y_2), when $\sigma_e(\vartheta_1)/Er^s = 1$. These functions represent (under a suitable normalization) the stress and the velocity fields. In Figs. 2–7 and Figs. 9–14 the angular distributions of the stress and velocity components are reported for $\alpha = 0.001$ and $\alpha = 0.1$, respectively. Various degrees of non-associativity are explored for the cases $\mu = 0.8$ (Figs. 2–7) and $\mu = 1.0$ (Figs. 9–14).

Table 1
Values of s, q and ϑ_1 ($\nu = 1/2$)

$\alpha = 0.001$				
μ	β	s	q	ϑ_1
0.8	0.8	−0.02394	17.65462	36.692
0.8	0.6	−0.03334	5.46313	29.650
0.8	0.4	−0.03861	3.37610	24.045
0.8	0.2	−0.04286	2.49603	19.133
0.6	0.6	−0.02431	5.33904	39.816
0.6	0.4	−0.03511	3.36579	31.294
0.6	0.2	−0.04155	2.49363	24.425
0.4	0.4	−0.02516	3.31713	43.445
0.4	0.2	−0.03789	2.48787	33.241
0.2	0.2	−0.02656	2.45930	47.770
0.2	0.1	−0.03557	2.20354	41.028
0.2	0.0	−0.04206	1.98923	35.616
0.1	0.1	−0.02751	2.18593	50.307
0.1	0.0	−0.03753	1.98404	43.038
0.0	0.0	−0.02866	1.96890	53.202

Table 2
Values of s, q and ϑ_1 ($\nu = 1/2$)

$\alpha = 0.1$				
μ	β	s	q	ϑ_1
1.0	1.0	−0.17914	12.61329	58.894
1.0	0.8	−0.18880	5.33852	58.543
1.0	0.6	−0.19902	3.49597	58.177
1.0	0.4	−0.21021	2.63698	57.804
1.0	0.2	−0.22292	2.12792	57.439
1.0	0.0	−0.23795	1.78210	57.122
0.8	0.8	−0.18497	4.92100	60.732
0.8	0.6	−0.19671	3.35213	60.457
0.8	0.4	−0.20928	2.57038	60.169
0.8	0.2	−0.22327	2.09179	59.881
0.6	0.6	−0.19302	3.18331	63.016
0.6	0.4	−0.20729	2.49038	62.822
0.6	0.2	−0.22285	2.04798	62.624
0.4	0.4	−0.20379	2.39237	65.826
0.4	0.2	−0.22130	1.99384	65.732
0.4	0.0	−0.24083	1.70125	65.653
0.2	0.2	−0.21810	1.92533	69.296
0.2	0.1	−0.22870	1.78478	69.313
0.2	0.0	−0.23991	1.65978	69.337
0.1	0.1	−0.22695	1.75279	71.342
0.1	0.0	−0.23883	1.63468	71.500
0.0	0.0	−0.23726	1.60583	73.646

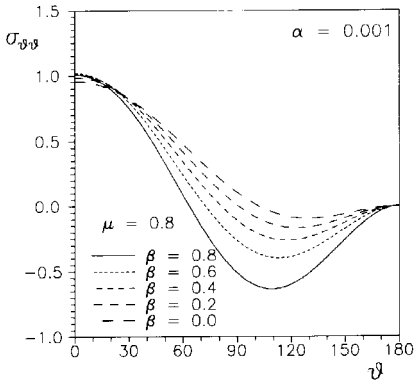

Fig. 2. Angular distribution of circumferential stress for small strain hardening and various degrees of non-associativity.

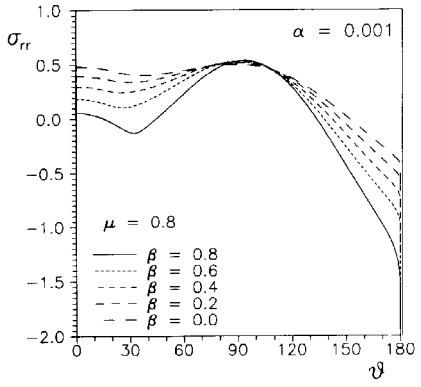

Fig. 3. Angular distribution of radial stress for small strain hardening and various degrees of non-associativity.

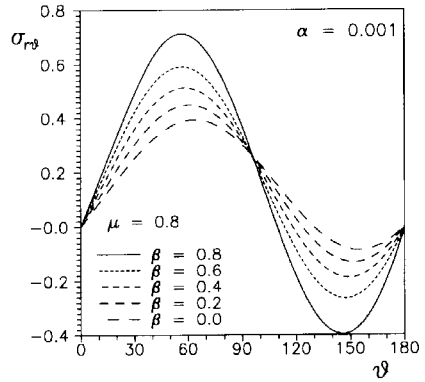

Fig. 4. Angular distribution of shear stress for small strain hardening and various degrees of non-associativity.

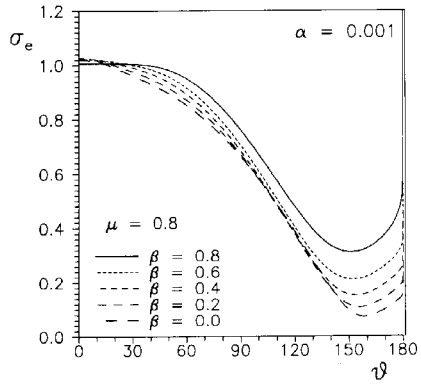

Fig. 5. Angular distribution of effective stress for small strain hardening and various degrees of non-associativity.

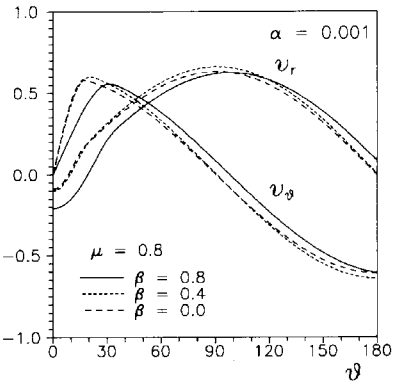

Fig. 6. Angular distribution of velocities in cyclindrical coordinates for small strain hardening and various degrees of non-associativity.

The qualitative trends of all curves are similar to the associative case. However, it is evident that the effect of non-associativity consists in a smoothing (increasing with the lowering of β/μ ratio) of the stress-component curves. The effect of non-associativity on the velocities is less evident. Moreover, by increasing α, all curves become close to each other and tend to the elastic solution. From Tables 1 and 2 it can be seen that *the non-associativity generally reduces the size of the plastic zone*. Notice that a similar effect is produced by the pressure-sensitivity (Bigoni and Radi, 1992). However, for high values of harden-

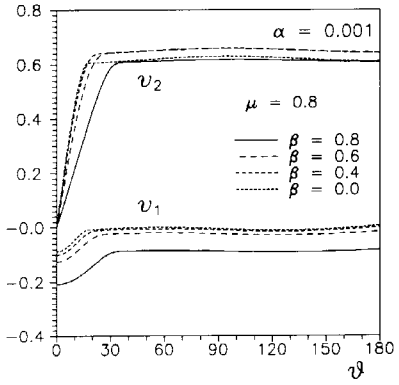

Fig. 7. Angular distribution of velocities in Cartesian coordinates for small strain hardening and various degrees of non-associativity.

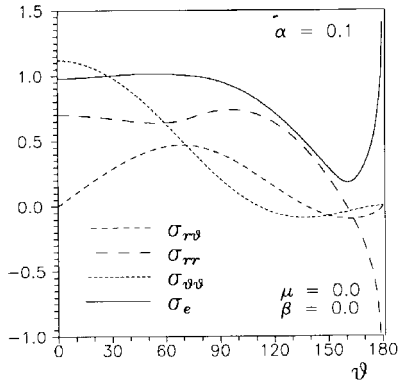

Fig. 8. Angular stress distribution for high strain hardening in the case of J_2-flow theory.

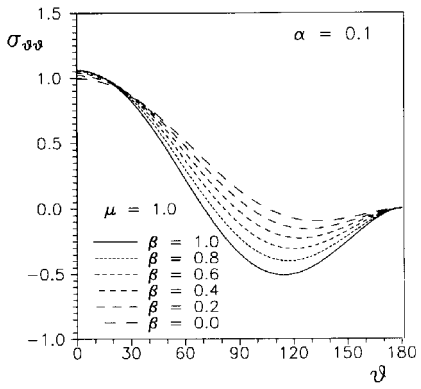

Fig. 9. Angular distribution of circumferential stress for high strain hardening and various degrees of non-associativity.

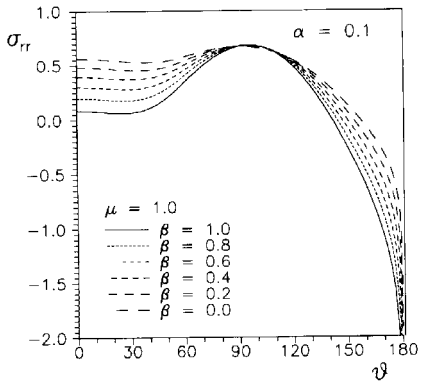

Fig. 10. Angular distribution of radial stress for high strain hardening and various degrees of non-associativity.

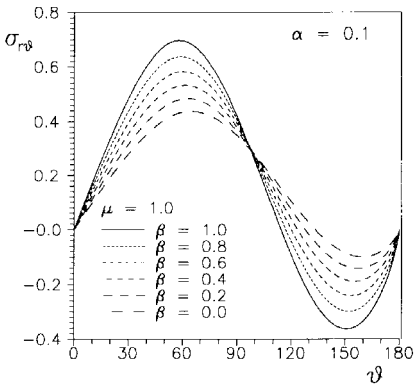

Fig. 11. Angular distribution of shear stress for high strain hardening and various degrees of non-associativity.

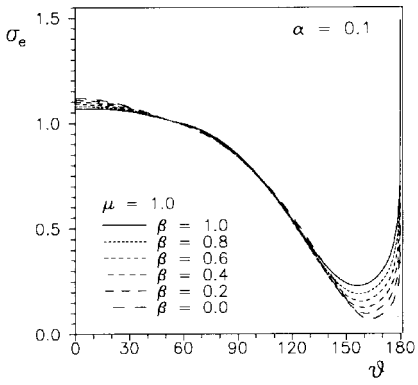

Fig. 12. Angular distribution of effective stress for high strain hardening and various degrees of non-associativity.

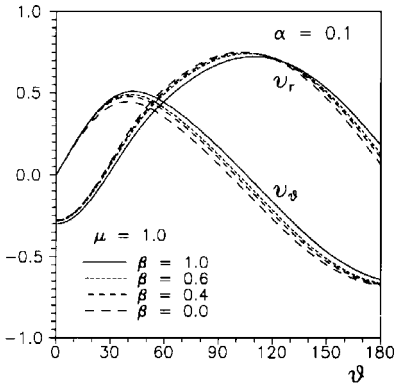

Fig. 13. Angular distribution of velocities in cylindrical coordinates for high strain hardening and various degrees of non-associativity.

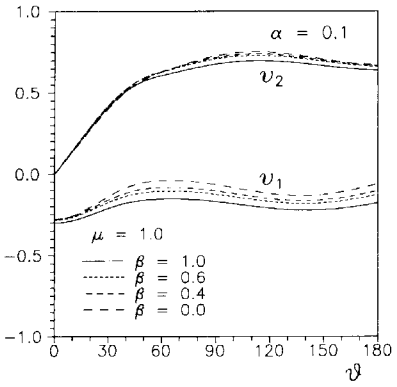

Fig. 14. Angular distribution of velocities in Cartesian coordinates for high strain hardening and various degrees of non-associativity.

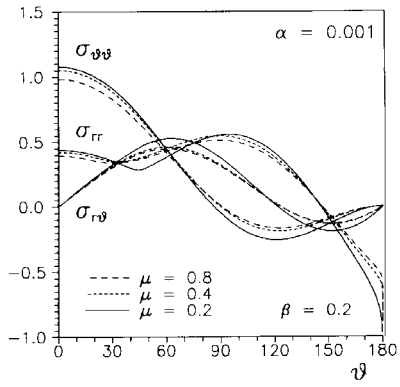

Fig. 15. Angular distribution of stress components for small strain hardening and various degrees of pressure-sensitivity.

ing, a slight opposite tendency is observed (in fact, for $\mu = 0.2$ and $\alpha = 0.1$ a slight increase in ϑ_1 is observed for a decreasing β). Moreover, the values of parameters s and q decrease with the ratio β/μ. In the associative case, it was shown in Bigoni and Radi (1992) that $\sigma_r(0) \to 0$ for small values of α ($= 0.001$), when μ approaches a value of approximately $\sqrt{3}/2$. The effect of the non-associativity opens the possibility of increasing μ well beyond $\sqrt{3}/2$ for small values of α, if β is kept sufficiently small (see, e.g., Table 3). In Figs. 15–18 solutions are reported corresponding to a constant value of β, for different values of μ (for $\alpha = 0.001$ and $\alpha = 0.1$). The plots of Figs. 15–18 reveal a remarkable feature, i.e., *a weak variation of fields (especially for the stress fields) with the pressure-sensitivity parameter μ, whereas a strong variation with the degree of non-associativity is observed*. Moreover, from the tables it appears evident that the *non-associativity controls the singularity s and the parameter q*. Therefore, for the

Table 3
Values of s, q and ϑ_1 for $\beta = 0.7$ ($\nu = 1/2$)

$\alpha = 0.001$			
μ	s	q	ϑ_1
1.3	−0.03782	8.40437	19.629
1.0	−0.03478	8.34921	25.906
0.9	−0.03276	8.30788	28.923
0.8	−0.02962	8.22896	32.710

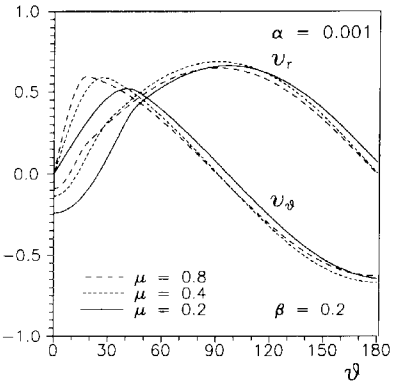

Fig. 16. Angular distribution of velocities in cylindrical coordinates for small strain hardening and various degrees of pressure-sensitivity.

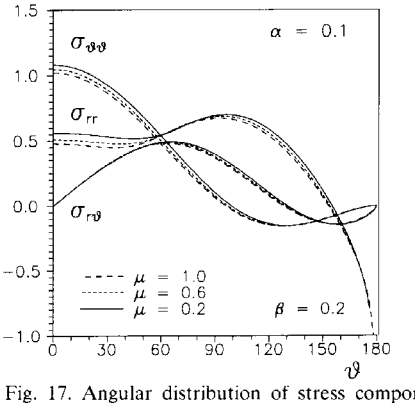

Fig. 17. Angular distribution of stress components for high strain hardening and various degrees of pressure-sensitivity.

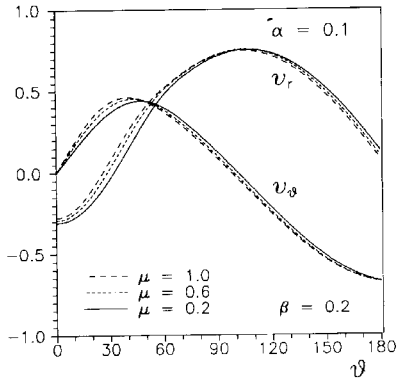

Fig. 18. Angular distribution of velocities in cylindrical coordinates for high strain hardening and various degrees of pressure-sensitivity.

assumed model, the crack fields appear to be governed by the flow-rule, rather than by the yield surface gradient.

5. Final discussion

The near tip fields of a steadily running crack in incremental elastoplastic solids with non-associative flow laws represents an almost unexplored aspect of fracture mechanics. The contribution of the present paper is restricted to a simple constitutive model, obeying the Drucker–Prager yield criterion with volumetric-non-associativity. Moreover, only the plane stress, small strains, quasi-static mode I has been analyzed. However, the results seem to change the scenario of the associative case substantially (see Bigoni and Radi, 1992; Li and Pan, 1990a,b; and Li, 1992 for the static case). In fact, the flow-rule appears to govern the near tip fields (especially the stress fields) and therefore a strong degree of non-associativity reduces the effect of pressure-sensitivity remarkably. In other words, the dependence of the stress fields on the pressure-sensitivity parameter is weak, whereas the dependence on the flow-rule is strong. However, at small strain hardening the plastic sector ahead the tip reduces in size with respect to the associative case. Moreover, an increasing in the non-associativity yields a stronger singularity of the fields. Therefore, *non-associativity represents an instabilizig effect in the crack growth*. It can be concluded that, in the analysis of crack propagation in pressure-sensitive solids, both the effects of pressure-sensitivity and non-associativity play an important role. Therefore, the non-associativity results to be an important parameter in crack propagation analyses, which deserves further theoretical and experimental investigations.

Acknowledgements

The financial support of the (Italian) Ministry of University and Scientific and Technological Research (MURST) and of the National Council of Research (CNR) is gratefully acknowledged.

References

Achenbach, J.D., M.F. Kanninien and C.H. Popelar (1981), Crack tip fields for fast fracture of an elastic–plastic material, *J. Mech. Phys. Solids 29*, 211–225.

Amazigo, J. and J.W. Hutchinson (1977), Crack-tip fields in steady crack-growth with linear strain hardening, *J. Mech. Phys. Solids 25*, 81–97.

Aoki, S., K. Kishimoto, A. Takeya and M. Sakata (1984), Effects of microvoids on crack blunting and initiation in ductile materials, *Int. J. Fract. 24*, 267–278.

Aoki, S., K. Kishimoto, T. Yoshida and M. Sakata (1987), A finite element study of the near crack tip deformation of a ductile material under mixed mode loading, *J. Mech. Phys. Solids 35*, 431–455.

Bigoni, D. (1992), Strain localization in axially-symmetric compression of brittle-cohesive materials, *Eng. Fract. Mech. 42*, 617–627.

Bigoni, D. and T. Hueckel (1990), A note on strain localization for a class of non-associative plasticity rules, *Ing. Arch. 60*, 491–499.

Bigoni, D. and E. Radi (1992), Mode I crack propagation in elastoplastic pressure-sensitive materials, *Int. J. Solids Struct.*, in printing.

Bigoni, D., and D. Zaccaria (1992), Strong ellipticity of comparison solids in elastoplasticity with volumetric non-associativity, *Int. J. Solids Struct. 29*, 2123–2136.

Chau, K.T. and J.W. Rudnicki (1990), Bifurcations of compressible pressure-sensitive materials in plane strain tension and compression, *J. Mech. Phys. Solids 6*, 875–898.

Chen, W.F. (1980), Constitutive relations for concrete, rock and soils: Discusser's report, Z.P. Bazant, ed., *Mechanics of Geomaterials*, Wiley, New York, pp. 65–86.

Chen, I.W. and P.E. Reyes-Morel (1986), Implications of transformation plasticity in ZrO_2-containing ceramics: I. Shear and dilatation effects, *J. Am. Ceram. Soc. 69*, 181–189.

Drucker, D.C. (1973), Plasticity theory, strength-differential (SD) phenomenon, and volume expansion in metals and plastics, *Metall. Trans. 4*, 667–673.

Drucker, D.C. and W. Prager (1952), Soil mechanics and plastic analysis or limit design, *Q. Appl. Math. 10*, 157–165.

Drugan, W.J. and J.R. Rice (1984), Restriction on quasi-statically moving surfaces of strong discontinuity in elastic–plastic solids, in: G.J. Dvorak and R.T. Shield, eds., *Mechanics of Material Behavior*, Elsevier, Amsterdam, pp. 59–73.

Drugan, W.J. and S. Yinong (1990), Finite deformation analysis of restrictions on moving strong discontinuity surfaces in elastic–plastic materials: Quasi-static and dynamic deformations, *J. Mech. Phys. Solids 38*, 553–574.

Drugan, W.J., J.R. Rice and T.L. Sham (1982), Asymptotic analysis of growing plane strain tensile cracks in elastic–ideally plastic solids, *J. Mech. Phys. Solids 30*, 447–473.

Gao, Y.C. (1987), Plane stress dynamic plastic field near a propagating crack tip, *Int. J. Fract. 34*, 111–129.

Gao, Y.C. and S. Nemat-Nasser (1983), Dynamic fields near a crack tip growing in an elastic–perfectly-plastic solid, *Mech. Mater. 2*, 47–60.

Gurson, A.L. (1977), Porous rigid–plastic materials containing rigid inclusions – yield function, plastic potential and void nucleation, (ICF4, Waterloo, Canada), *Fracture 2*, 357–364.

Horii, H. and S. Nemat-Nasser (1982), Instability of a half-space with frictional materials, *J. Appl. Math. Phys. (ZAMP) 33*, 1–16.

Huang, Y., J.W. Hutchinson and V. Tvergaard (1991), Cavitation instabilities in elastic plastic solids, *J. Mech. Phys. Solids 39*, 223–241.

Hutchinson, J.W. (1968a), Singular behaviour at the end of a tensile crack in a hardening material, *J. Mech. Phys. Solids 16*, 13–81.

Hutchinson, J.W. (1968b), Plastic stress and strain fields at a crack tip, *J. Mech. Phys. Solids 16*, 337–347.

Hutchinson, J.W. and V. Tvergaard (1980), Surface instabilities on statically strained plastic solids, *Int. J. Mech. Sci. 22*, 339–354.

Jenike, A.W. and R.T. Shield (1959), On the plastic flow of Coulomb solids beyond original failure, *J. Appl. Mech. 26*, 599–602.

Li, F.Z. (1992), The analytic solution of near tip stress fields for perfectly plastic pressure-sensitive material under plane stress condition, *Int. J. Fract. 53*, 325–336.

Li, F.Z. and J. Pan (1990a), Plane-strain crack-tip fields for pressure-sensitive dilatant materials, *J. Appl. Mech. 57*, 40–49.

Li, F.Z. and J. Pan (1990b), Plane-stress crack-tip fields for pressure-sensitive dilatant materials, *Eng. Fract. Mech. 35*, 1105–1116.

Lo, K.K. (1979), Modeling of plastic yielding at a crack tip by inclined slip planes, *Int. J. Fract. 15*, 583–589.

Mandel, J. (1966), Conditions de stabilite et postulat de Drucker, J. Kravtchenko and P.M. Sirieys, eds., *Rheology and Soil Mechanics*, Springer, Berlin, pp. 58–68.

Mróz, Z. (1963), Non-associated flow laws in plasticity, *J. Mec. II*, 21–42.

Narasimhan, R. and A.J. Rosakis (1987), Reexamination of jumps across quasi-statically propagating surfaces under generalized plane stress in anisotropically hardening elastic–plastic solids, *J. Appl. Mech. 54*, 519–524.

Needleman, A. (1979), Non-normality and bifurcation in plane strain tension or compression, *J. Mech. Phys. Solids 27*, 231–254.

Needleman, A. and J.R. Rice (1978), Limits to ductility set by plastic flow localization, D.P. Koistinien and N.M. Wang, eds., *Mechanics of Sheet Metal Forming*, Plenum Press, New York, pp. 237–267.

Needleman, A. and V. Tvergaard (1987), An analysis of ductile rupture modes at a crack, *J. Mech. Phys. Solids 35*, 151–183.

Needleman, A. and V. Tvergaard (1992), Effect of crack meandering on dynamic, ductile fracture, *J. Mech. Phys. Solids 40*, 447–471.

Nemat-Nasser, S. and Y.C. Gao (1988), Discontinuities in elastic–plastic solids, *Mech. Mater. 7*, 215–229.

Nemat-Nasser, S. and M. Obata (1990), Some basic issues in dynamic crack growth in elastic–plastic solids, *Int. J. Fract. 42*, 287–300.

Nemat-Nasser, S. and A. Shokooh (1980), On finite plastic flows of compressible materials with internal friction, *Int. J. Solids Struct. 16*, 495–514.

Östlund, S. and P. Gudmundson (1988), Asymptotic crack tip fields for dynamic fracture of linear strain-hardening solids, *Int. J. Solids Struct. 24*, 1141–1148.

Palaniswamy, R. and S.P. Shah (1974), Fracture and stress–strain relationship of concrete under triaxial compression, *J. Struct. Eng., ASCE, ST5(100)*, 901–916.

Ponte-Castañeda, P. (1987a), Asymptotic fields in steady crack growth with linear strain-hardening, *J. Mech. Phys. Solids 35*, 227–268.

Ponte-Castañeda, P. (1987b), Plastic stress intensity factors in steady crack growth, *J. Appl. Mech. 54*, 379–387.

Ponte-Castañeda, P. and P.A. Mataga (1991), Stable crack growth along a brittle/ductile interface – I. Near-tip fields, *Int. J. Solids Struct. 27*, 105–133.

Reyes-Morel, P.E. and I.W. Chen (1988), Transformation plasticity of CeO_2-stabilized tetragonal zirconia polycrystals: I. Stress assistance and autocatalysis, *J. Am. Ceram. Soc. 71*, 343–353.

Rice, J.R. (1976), The localization of plastic deformation, in: Z.P. Bazant, ed., *Theoretical and Applied Mechanics*, North-Holland, Amsterdam, pp. 207–220.

Rice, J.R. (1980), Shear localization, faulting, and frictional slip: Discusser's report, Z.P. Bazant, ed., *Mechanics of Geomaterials*, Wiley, New York, pp. 211–216.

Rice, J.R. (1982), Elastic–plastic crack growth, in: H.G. Hopkins and M.J. Sewell, eds., *Mechanics of Solids: The Rodney Hill 60th Anniversary Volume*, Pergamon Press, Oxford, pp. 539–562.

Rice, J.R., W.J. Drugan and T.L. Sham (1980), Elastic–plastic analysis of growing cracks, *Fract. Mech., ASTM-STP 700*, 189–219.

Rice, J.R. and G.F. Rosengren (1968), Plane strain deformation near a crack tip in a power-law hardening material, *J. Mech. Phys. Solids 10*, 1–12.

Riedel, H. (1976), Plastic yielding on inclined slip-planes at a crack tip, *J. Mech. Phys. Solids 24*, 277–289.

Rittel, D. (1990), The influence of microstructure on the macroscopic patterns of surface instabilities in metals, *Scr. Metall. Mater. 24*, 1759–1764.

Rudnicki, J.W. and J.R. Rice (1975), Conditions for the localization of deformations in pressure-sensitive dilatant materials, *J. Mech. Phys. Solids 23*, 371–394.

Slepyan, L.I. (1974), Growing crack during plane deformation of an elastic plastic body, *Mekh. Tverd. Tela 9*, 57–67.

Spitzig, W.A., R.J. Sober and O. Richmond (1976), The effect of hydrostatic pressure on the deformation behavior of maraging and HY-80 steels and its implications for plasticity theory, *Metall. Trans. 7A*, 1703–1710.

Torrenti, J.M. and E.H. Benaija (1990) Stereophotogrammetry: A new way to study strain localization in concrete under compression, *9th Conf. on Experimental Mechanics*, Lyngby, Copenhagen.

Vardoulakis, I. (1981), Bifurcation analysis of the plane rectilinear deformation on dry sand samples, *Int. J. Solids Struct. 11*, 1085–1101.

Vitek, V. (1976), Yielding on inclined planes at the tip of a crack loaded in uniform tension. *J. Mech. Phys. Solids 24*, 263–275.

Whitney, W. and R.D. Andrews (1967), Yielding of glassy polymer: Volume effects, *J. Polym. Sci., Part C, 16*, 2981–2990.